70.1: LED-Illuminated Pico Projector Architectures

Denis Darmon, John R. McNeil, and Mark A. Handschy
Displaytech, Inc., Longmont, Colorado, USA

Abstract
Optical architecture choices optimize pico-projection engines for battery-powered embedded applications and wall-plug-powered stand-alone applications. Embedded engines offer power efficiencies above 6 lm/W, while stand-alone systems offer luminous outputs up to 110 lm.

1. Introduction
Access to large-screen visual content via small mobile devices, particularly in connected applications, presents a problem that can be solved by pico-projectors that cast a large-diagonal, high resolution image from a highly miniaturized engine [1]. Pico projector applications can be divided into distinct segments: (1) embedded, (2) companion, and (3) stand-alone. In the embedded segment, where the engine resides inside the mobile device, power consumption and engine size will be the most important performance criteria. In the stand-alone segment, on the other hand, total light output will be most important. Separate companion projectors, with their own batteries but that connect to mobile platforms, will have intermediate size and light output. Single-panel, sequential-color engines enabled by fast-switching ferroelectric-liquid-crystal-on-silicon (FLCOS) panels provide an attractive basis for pico projectors [2], offering high optical efficiency and an ultra-compact low-power electronic system [3]. Herein we present exemplary optical architectures based on LED color-sequential illumination of a single FLCOS microdisplay panel, some targeted for each of the battery-powered embedded, companion, and stand-alone segments. The embedded engines offer power efficiencies above 6 lm/W, while companion and stand-alone engines offer luminous outputs of 18 and up to 110 lm, respectively.

2. System Configurations
Figure 1 shows two example pico-projection optical system configurations. System I in Figure 1(a) has the simplest optical architecture, favoring the highest degree of miniaturization needed for embedded application. Light from four LED die (RGGB), packaged on a single substrate, is collected and collimated by a single optic. A holographic diffuser or lenticular element and lenses convert the inhomogeneous round beam to a uniform rectangular spot on the microdisplay. System II in Figure 1(b) uses separate red, green, and blue LEDs superimposed with dichroic filters to minimize effective source area, favoring the use of a polarization conversion system (PCS) to give the highest light output. The optical configurations of Figure 1 are meant to illustrate key concepts rather than realistic designs. With regard to the illumination optics in particular there are a wide variety of design options [4, 5], only a few of which are illustrated. For example, light emitted from the LED could be collected by an all-refractive optic as in Figure 1(a), a combination refractive and reflective optic (b) or by a CPC (compound parabolic concentrator), perhaps with rectangular cross section (not shown). Uniform, efficient illumination of the display panel can be obtained by using tailored diffusers (a), fly's-eye lenslet arrays (b), or by imaging either the output of a rectangular rod integrator or a rectangular LED directly onto the panel (not shown). Polarization efficiency can be boosted by reflecting the unused polarization back through some scrambling or rotating element onto the LED die which again reflects some portion of the light back towards the panel (polarization *recycling*). Alternately, unpolarized light emitted by the LED can be split into its two components by a polarizing beam splitter (PBS). The polarization of one component is then rotated by a wave plate prior to its recombination with the other to form a single beam (polarization *conversion*).

In spite of the diversity of system design choices there are fundamental limitations on achievable system light output independent of the design. The optical Brightness Theorem dictates a size scale for light sources used in projection displays. The maximum useful light-source area A_S shares a relationship with the display panel area A_P and the acceptance angle θ_P of the optical system, according to equation (1):

$$A_S \sin^2\theta_S < A_P \sin^2\theta_P. \quad (1)$$

The example of a hypothetical lambertian LED light source with Displaytech's 0.46-inch diagonal SVGA FLCOS panel helps clarify these limitations. The lambertian source emits uniformly into a hemisphere ($\theta_S = 90°$). The 0.46-inch display panel (A_P = 73 mm^2 with 5% overfill in horizontal and vertical directions) projects an image through an $f/2$ projection lens ($\sin\theta_P = 0.25$).

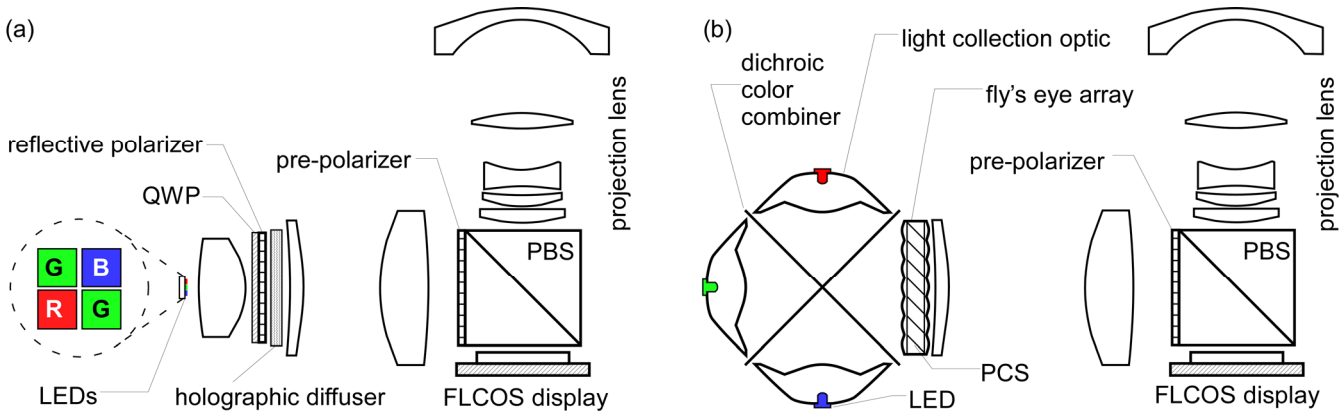

Figure 1. Example pico-projection optical systems: (a) System I, (b) System II.

ISSN0097-966X/06/3701-0000-$1.00+.00 © 2009 SID

Therefore, the maximum useful LED area A_S is 4.6 mm^2, equivalent to an LED emission area of about 2.1 × 2.1 mm. Using more or larger LEDs cannot raise the image brightness for a display panel of this size and an optical system of this speed. We now describe the characteristics of the key engine components prior to estimating projection system light budgets.

3. Key Components

3.1. FLCOS Microdisplay

Displaytech's FLCOS panels provide the fast switching needed for single-panel sequential color, without the usual electronic-system complexity associated with re-ordering standard video data [3]. Table 1 shows optical throughput measurements, as described in Section 6, for early engineering samples of Displaytech's LV-SVGA panel. Throughput is essentially independent of numerical aperture (NA); FLCOS cell gap choice maximizes throughput in the green with throughput in the blue and red slightly lower. Here, color throughputs are representative of all-white throughput, unlike in color-filter-array (CFA) panels where fringing-field effects dim saturated-color content relative to all-white. Figure 2 shows contrast ratio results. Circles represent contrast obtained for each LED primary color with the beam splitter in collimated light, while the diamonds shows photopically weighted white-light contrast with the beam splitter in converging light. Comparing these two indicates the degree to which the in-plane quarter-wave retardance of the FLCOS OFF state compensates for skew-ray depolarization on the PBS.

Table 1. FLCOS panel ON-state reflectance.

PANEL	GREEN	RED	BLUE	PHOTOPIC
1	0.67	0.56	0.62	0.64
2	0.68	0.56	0.64	0.64
3	0.64	0.54	0.58	0.61
4	0.63	0.53	0.58	0.60

3.2. Polarizing Beam Splitters

The ideal polarizing beam splitter (PBS) for a single-panel pico projector would provide high round-trip optical throughput for all colors, and over a large range of angles, to enable small micro-display panels to work with relatively large light sources. Three technologies could provide these characteristics: (1) dielectric coatings (MacNeille), (2) wire-grid arrays, and (3) birefringent film stacks such as 3M's "multi-layer optical film" (MOF).

Figure 3 shows our measurements made as described in Section 6 of a MacNeille PBS, manufactured from SF57 glass by Foreal

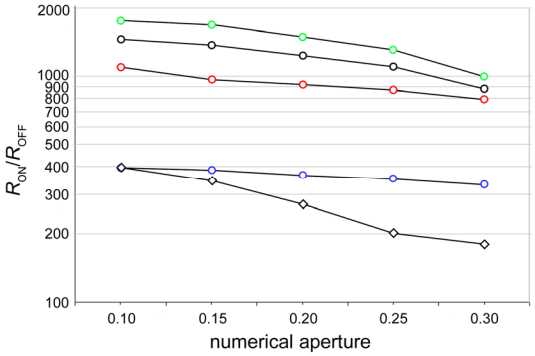

Figure 2. FLCOS panel contrast vs. NA. Circles: Figure 5(a) setup, LED primary colors and (black) photopic weighting of color values (panel orientation fixed at optimum for green). Diamonds: Figure 5(b) setup, white light, photopic detector.

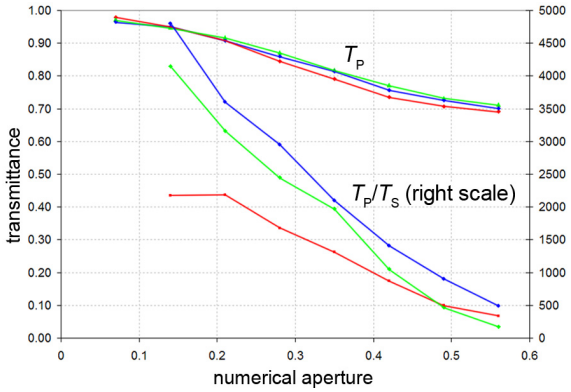

Figure 3. MacNeille PBS properties for LED primary colors

Spectrum, Inc (San Jose, CA). This PBS offers optical throughput essentially independent of wavelength, with ⟨*p*⟩ transmittance T_P as shown and ⟨*s*⟩ reflectance R_S (not shown) about 0.98 up to NA 0.5. Transmitted-beam contrast in all colors remains greater than 1000:1 down to *f*/1.2. Round-trip throughput ($R_S \cdot T_P$) is about 86% at *f*/2. Measurements on a PBS made by Unaxis (now Oerlikon Optics, Golden, CO) from less-expensive SF2 glass gave similar broad spectrum results, but over a slightly narrower angle range as expected for the lower-index glass.

Wire-grid and birefringent polymer film polarizers also offer broad-spectrum wide-angle performance. Characterization by Yu and Kwok [6] of wire-grid polarizers commercially available from Moxtek (Orem, UT) indicate that round-trip throughput of about 0.78 can be obtained at *f*/2. According to work by Magarill and Bruzzone, MOF polarizers from 3M (St. Paul, MN) offer $T_P \approx 0.97$ and $R_S \approx 0.95$ at speeds as fast as *f*/1.9 (round-trip throughput about 0.92), with contrast ratios approaching 10000:1 [7]. Table 2 compares PBS optical throughput characteristics.

Table 2. PBS round-trip throughput at *f*/2.

MOF*	MacNeille†	MacNeille‡	wire-grid§
0.92	0.86	0.83	0.78

*ref. [7]; †Foreal Spectrum, ‡Unaxis, §ref. [6]

3.3. LEDs, White Balance, and Duty Cycle

Our estimates of light flux available for projector illumination can be understood from an example portrayed in Table 3, based on the Osram Diamond Dragon LEDs. Lines 2–4 show data sheet values for light output and nominal drive currents. Reduced duty cycles pertinent to sequential color permit higher drive currents (line 5), giving corresponding higher light outputs (line 6). For 60 Hz input video, with 2× color-rate multiplier, a complete RGB color cycle lasts 8.33 ms (line 10). Relative durations of red, green, and blue fields (lines 11, 12) are adjusted to give a desired white balance at the allowed pulse drive currents. The FLCOS panel employs pulse width modulation [3]: all pixels are written ON at the beginning of each field, with the illumination held off for a blanking time (line 13) slightly longer than the FLC response time (line 14) to allow black pixels to attain their OFF state. For DC balance current FLCOS panels require 50% of the duty cycle be devoted to an inverse image with illumination blanked, resulting in the net LED on-times shown in line 15, leading directly to the LED light outputs in lines 17 and 18. The total LED light output serves as the input to the projector light budget in Table 4. For completely linear gray scale, illumination stays on until even full-bright pixels have switched OFF; the light loss (half of an FLC switching time) is accounted for in the "temporal fill factor" on line 19.

Table 3. LED light output for Osram Diamond Dragon.

	PARAMETER	UNIT	RED	GRN	BLU
1	part # L*X* W5AP		A	T	B
2	typical light output	lm	185	210	71
3	nominal drive current	A	1.40	1.40	1.40
4	nominal forward voltage	V	2.5	3.5	3.5
5	pulse current	A	2.85	2.50	3.00
6	pulse output	lm	**314**	**353**	**128**
7	pulse forward voltage	V	2.75	3.85	3.90
8	frame rate	Hz		60	
9	Rate multiplier			2	
10	cycle time	ms		8.33	
11	R:G:B duration ratio		0.27	0.50	0.23
12	R:G:B field durations	ms	2.25	4.17	1.92
13	LED blanking	ms	0.17	0.16	0.17
14	FLC response time	ms	0.15	0.15	0.15
15	LED on-time	ms	0.96	1.92	0.79
16	FLC duty cycle		0.92	0.96	0.90
17	average LED light output	lm	36	81	12
18	average total light output	lm		**129**	
19	average temporal "fill factor"			0.94	
20	average illum. duty cycle			0.44	
21	average power consumption	W	0.90	2.22	1.11

While Table 3 assumes only one LED color is active during each color field, producing highly saturated primary colors, multiple LED colors can be mixed during a given color field to produce higher light output [8]. Figure 4 shows the native LED gamut (outer triangle), and a reduced gamut corresponding to our measurements of a white-LED-illuminated color-filter array (CFA) LCOS display [9] (inner triangle). When we matched this smaller gamut with color-sequential illumination (while keeping color field durations, LED on-times, and maximum LED drive levels as listed in Table 3) we measured a 147% increase in illuminator output, from 4054 lx to 5953 lx, with no shift in white point (central circle and overlapped square).

Recently developed bistable FLC devices [10] eliminate the above mentioned need for inverse-image blanking, allowing FLCOS microdisplays to be illuminated for the full frame time, and raise illumination duty cycle (Table 3, line 20) from 44% to 94% for the same color field rate and LED blanking times.

4. Pico Projector Light Budgets

The measured optical throughput characteristics of the PBS and FLCOS display panel, along with LED light outputs achievable with color sequential operation, provide the inputs to the overall projector light budgets in Table 4, which uses several different LED configurations to achieve different light outputs. The estimates share common assumptions about polarization, reflection, and overfill losses. A 43% transmissive dichroic film coupled with 86% PBS round-trip throughput gives a 37% polarization throughput factor for unpolarized input light. FLCOS panel R_{ON} of 60%, a four-element projection lens transmitting 92% (1% loss per surface), and estimated coupling efficiency of 80% for the illumination optics give a reflection throughput factor of 44%. Overfilling the 66 mm^2 active area of Displaytech's LV-SVGA panel by 5% in each linear dimension produces an illuminated spot area of 73 mm^2, giving a throughput factor of 91%.

The LED die area, the refractive index of its encapsulating lens (if any), and whether or not the optical system superimposes the different LED colors determines the effective light source area,

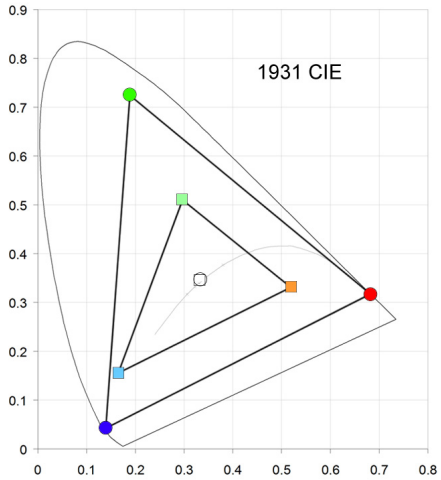

Figure 4. Native LED and color-mixing-reduced gamuts.

and hence the minimum system NA and *f*/#. The Osram OSTAR (choice A) offers four LEDs on a single substrate, avoiding the optical losses associated with color combination (which we here estimate at a throughput of 0.8), but at the penalty of a larger source area which may preclude the use of PCS. Krijn et al. have shown 27% gain, however, for simple polarization recycling, and predicted gains as high as 54% with improved LEDs [11]; here we estimate 20%. Lumileds Rebel LEDs (choice B), achieve higher efficacy through molded encapsulation; the color superposition of the more complex System II optics still keeps the effective source area small enough for PCS (estimated gain for unpolarized light

Table 4. Pico projector light budgets for various LED choices.

LED CHARACTERISTICS					
LED choice	A*	B†	C‡	D§	E#
die height (mm)	2.1	1	1.35	1.71	2
die width (mm)	2.1	1	1.6	2.28	2.7
die area (mm^2)	4.4	1.0	2.2	3.9	5.4
encap. ref. index	1.0	1.5	1.42	1.0	1.0
effective area (mm^2)	4.4	2.3	4.4	3.9	5.4
duty ratio R:G:B	35/33/33	30/40/30	27/50/23	34/38/29	34/38/29
illum. duty cycle	0.44	0.44	0.44	0.44	0.94
illum. power (W)	2.14	1.42	4.2	14.3	42
optical system	I	II	II	II	II
LED white flux (lm)	45	47	129	245	795
COMMON THROUGHPUT FACTORS					
polarization			0.37		
reflection			0.44		
panel overfill			0.91		
DIFFERENTIATING THROUGHPUT FACTORS					
pol. recycling	1.2		1.2	1.2	1.2
PCS		1.7			
color combination		0.8	0.8	0.8	0.8
temporal "fill factor"	0.94	0.94	0.94	0.94	0.97
TOTALS					
total t'put factor	0.167	0.191	0.135	0.135	0.139
output (lm)	**7.5**	**9.0**	**17.4**	**33**	**110**
efficiency (lm/W)	**3.5**	**6.3**	**4.1**	**2.3**	**2.6**
system NA	0.25	0.25	0.24	0.23	0.27
system f/#	2.0	2.0	2.0	2.2	1.8

*Osram OSTAR (RGGB); †Lumileds Rebel; ‡Osram Diamond Dragon; §Luminus PT39; #Luminus PT54.

of 1.7) at *f*/2, giving efficiency of 6.3 lm/W, the highest of any of our examples. Substituting the larger Osram Diamond Dragon LEDs (choice C) enables an output of nearly 18 lm, appropriate for a companion projector. With an *f*/1.5 projection lens, PCS could be substituted for recycling, boosting output to 25 lm.

Finally, we contemplate two stand-alone systems with large, high-output Luminus Phlatlight LEDs. Today's FLCOS panels could provide 33 lm output with the smaller PT39 LEDs (choice D), while with next-generation bistable panels and the larger PT54 LEDs (choice E), achievable output jumps past the 100-lm mark.

5. Conclusions

The pico projection systems envisioned here are optimized for the varying requirements of embedded, companion, and stand-alone mobile applications, as summarized in Table 5. Embedded engines could deliver light outputs approaching 10 lm with power consumptions only slightly over 1 W, providing 150 cd/m^2 brightness on an 8-inch diagonal screen. High-output stand-alone engines could provide the same image brightness on a 27-inch screen. Pico projectors with these characteristics will facilitate personal and shared viewing of high resolution images in situations where flat-panel displays on mobile devices are too small.

Table 5. Pico projector summary (including achievable screen diagonal at 150 cd/m^2).

	SEGMENT	FEATURE	OUT (lm)	POWER (W)	EFF. (lm/W)	DIAG. (in).
A	embedded	compact	7.5	2.1	3.5	7.2
B	embedded	efficient	9.0	1.4	6.3	7.8
D	companion	bright	17.8	4.4	4.1	11
E	std-alone	brightest	110	42	2.6	27

6. Appendix: Optical Measurements

We characterized panel and PBS optical properties using the setups shown in Figure 5. Panel optical throughput was characterized by measuring ON-state reflectance R_{ON} using the setup shown in Figure 5(a). Light from an LED-illuminated integrating rod is collected and collimated by a first achromat, polarized, and reflected off a beam splitter to be focused onto the panel under test by a second achromat; an iris at the shared back focal plane of the two lenses controls the numerical aperture (NA) of the light incident on the panel. Light reflected by the panel is transmitted through the beam splitter, analyzed, and focused onto a detector by an aspheric condenser. A second iris provides separate control over the collection NA. Using the dichroic polarizer to set the incident-light polarization accurately perpendicular to the plane of incidence ensures a high instrument extinction ratio (several thousand to one). Throughput calibration relies on the detector reading obtained with a high reflectance mirror substituted for the panel with the analyzer parallel to the polarizer. Readings obtained with the panel are then normalized to the mirror reading, and corrected for the mirror reflectance (~99%) and the ratio of the beam splitter transmittances for $\langle p \rangle$ and $\langle s \rangle$ light ($T_P/T_S \sim 1.187$).

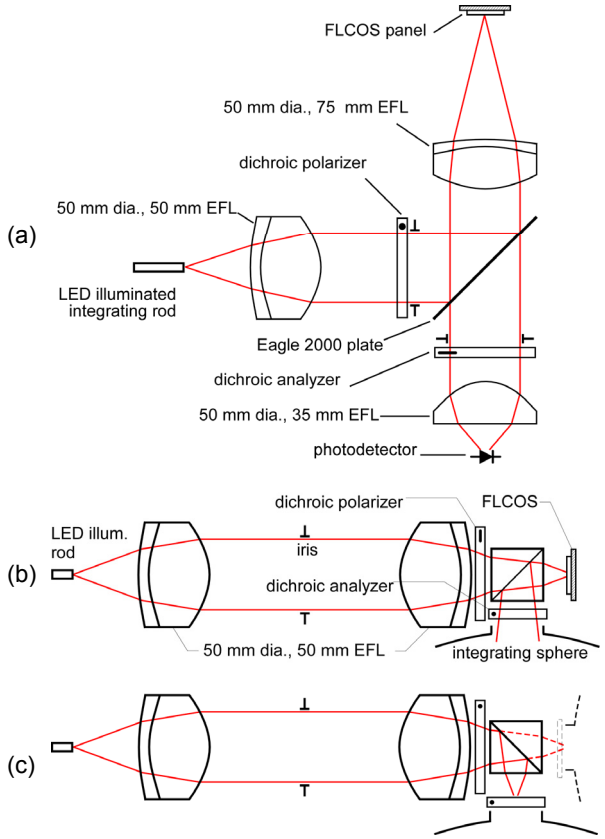

Figure 5. Optical test setups: for panel with beam splitter in (a) collimated and (b) converging light; (c) for PBS.

7. References

[1] W. Coggshall, M. Abramson, C. Hogan, and A. Poor, "New era: a sea change in the front-projection industry," Information Display **23**, 34–38 (2007).

[2] M. A. Handschy, "Moves toward mobile projectors raise issue of panel choice," Display Devices **48**, 6–8 (2007).

[3] M. A. Handschy and J. Dallas, "Scalable sequential-color display without ASICs," SID Symposium Digest **38**, 109–112 (2007).

[4] Edward H. Stupp and Matthew S. Brennesholtz, *Projection Displays* (Wiley, Chichester, 1999).

[5] M. G. Robinson, J. Chen, and G. D. Sharp, *Polarization Engineering for LCD Projection* (Wiley, Chichester, 2005).

[6] X. J. Yu and H. S. Kwok, "Application of wire-grid polarizers to projection displays," Appl. Opt. **42**, 6335–6341, (2003).

[7] S. Magarill and C. L. Bruzzone, "Detailed optical characteristics of multi-layer optical film polarization beam splitter," J. Soc. Info. Display **15**, 811–816 (2007).

[8] M. H. Keuper, G. Harbers, and S. Paolini, "RGB LED illuminator for pocket-sized projectors," SID Symposium Digest **35** 943–945 (2004).

[9] H. C. Huang, B. Zhang, H. Peng, H. S. Kwok, P. W. Cheng, and Y. C. Chen, "Processes, characterizations, and system applications of color-filter liquid-crystal-on-silicon microdisplays," J. Soc. Info. Display **14**, 499–508 (2006).

[10] M. J. O'Callaghan, R. Ferguson, R. Vohra, et al., "Bistable FLCOS devices for doubled-brightness micro-projectors," SID Symposium Digest **39**, 232–235 (2008).

[11] M. P. Krijn, B. A. Salters, and O. H. Willemsen, "LED-based mini-projectors," Proc. SPIE **6196**, 619602–619614, (2006).